Contents lists available at ScienceDirect

Energy

journal homepage: www.elsevier.com

Impact of EV penetration in the interconnected urban environment of a smart city

C.F. Calvillo*, A. Sánchez-Miralles, J. Villar, F. Martín

Institute for Research in Technology (IIT), ICAI School of Engineering, Comillas Pontifical University, Santa Cruz de Marcenado 26, 28015, Madrid, Spain

ARTICLE INFO

Article history:
Available online xxx

Indexterms:
Demand response
Distributed energy resources
Electric vehicle
Energy management
Public transport systems
Smart city

ABSTRACT

The smart city seeks a highly interconnected, monitored and globally optimized environment to profit from the synergies among systems such as energy, transports or waste management. From an energy perspective, transport systems and facilities are among the bigger energy consumers inside cities. However, despite the research available on such systems, few works focus on their interactions and potential synergies to increase their efficiencies.

This paper address this problem by assessing the benefits of the interconnection and joint management of different energy systems in a smart city context. This is done using a linear programming problem, modelling a district with residential loads, distributed energy resources (DER) and electric vehicles (EV), which are also connected to an electrical metro substation. This connection allows to store the metro regenerative braking energy into EVs' batteries to be used later for other trains or for the EVs themselves. The objective of the linear programming model is to find the optimal planning and operation of all the considered systems, achieving minimum energy costs.

Therefore, the main contributions of this paper are the assessment of synergies of the interconnection of these systems and the detailed analysis of the impact of different EV penetration levels. Results show important economic benefits for the overall system (up to 30%) when the investments and its operation are globally optimized, especially reducing the metro energy costs. Also, analysing the energy transfers between metro-EV, it is evident that the metro takes advantages of the cheaper energy coming from the district (through the EVs), showing the existence of "opportunistic" synergies. Lastly, EV saturation points (where extra EVs represent more load but do not provide additional useful storage to the system) can be relatively small (200–300 EVs) when the energy transfer to the metro electrical substation is restricted, but it is also reduced by the presence of DER systems.

Nomenclature

Sets

c, v	Type of houses (1–4) and EV users (1,2)
h	Hour (1–24)
hMs, hMw	Summer and winter mid-peak hours for time-of-use tariffs
hO	Off-peak hours for the electric time-of-use tariffs
hPs, hPw	Summer and winter peak hours for the time-of-use tariffs
mS, mW, m	Summer (3–8), winter (1,2,9–12) and all months (1–12)
y	Years (1 – lifespan)

Parameters

$pAvailEV_{v,h}$	Max. available capacity of EVs (kWh)
$pBuyEpriceH_{m,h}$, $pBuyEpriceM_{m,h}$	Electricity base residential and commercial prices (€/kWh)
pCOP	Coeff. of Performance for HP
pCostBat	Total upfront cost of batteries, considering a replacement every 8 years (€/MWh)
pCostPV, pCostHP	Total cost per installed Watt of PV and HP (€/MW)
$pCostT_y$, $pCostE_y$	Annual buying price increment of thermal and electric energy (%)
$pSellE_y$	Annual selling price increment of electric energy (%)
$pDaysM_m$	Number of days in month *m*
$pDemandElec_{c,m,h}$	Base electric demand curve for 12 representative days (MWh)
pDemandShift	Maximum allowed load to be shifted per day of the base electric demand (%)
$pDemandTherm_{c,m}$	Total thermal demand for 12 representative days (MWh)
$pGHI_{m,h}$	Global horizontal irradiance (W/m2)
pDRequipCost	Costs of equipment required to do load shifting (€/client)
pEffBat	Battery charge/discharge efficiency (%)
pEVcap	Max. storage capacity per EV (kWh)
pFixEpow, pFixTpow	Annual access tariff for residential electric and thermal power (€/kW, €/client)

* Corresponding author.
Email addresses: christian.calvillo@iit.comillas.edu (C.F. Calvillo); alvaro@comillas.edu (A. Sánchez-Miralles); jose.villar@iit.comillas.edu (J. Villar); francisco.martin@iit.comillas.edu (F. Martín)

https://doi.org/10.1016/j.energy.2017.12.006
0360-5442/

$pHouseNum$, $pEVnum$ Number of equivalent clients per house and EV user types
$pLifespan$ Expected lifespan for PV and HP systems in the study (20 years)
$pLossesPV$, $pLossesHP$ Total losses in the PV and HP systems (%)
$pMetLoad_h$, $pMetReg_h$ Base electric demand curve and regenerative braking energy for the metro trains connected to the substation (kWh)
$pOMfixPV$, $pOMfixHP$ Fixed annual operation and maintenance costs per installed Watt of PV and HP (€/MW)
$pPeakPowM$, $pMidpPowM$, $pOffpPowM$ Annual access tariff for commercial (metro) electric power at peak, mid-peak and off-peak hours (€/kW)
$pSellEpriceH$ Electricity base selling price (€/kWh)
$pSOCinitEV_{v,h}$ SOC of the arriving EV (%)
$pSOCminEV_{v,h}$ Minimum SOC requirement for EV (%)

Positive variables

$vBatCap_c$ Battery installed capacity(MWh)
$vChBat_{c,m,h}$, $vDisBat_{c,m,h}$ battery charged/discharged Energy (MWh)
$vChEV_{v,m,h}$, $vDisEV_{v,m,h}$ Energy charged/discharged to/from EV (MWh)
$vChMetro_{v,m,h}$, $vDisMetro_{v,m,h}$ Energy charged/discharged from EV to the metro system (MWh)
$vDecDemand_{c,m,h}$ Decrease in base demand(MWh)
$vDemandNew_{c,m,h}$ New consumption curve after changing the base profile (MWh)
$vGridEnBuy_{m,h}$ $vGridEnSell_{m,h}$ Total energy transaction to the grid (buying and selling) (MWh)
$vHPenInput_{c,m,h}$ Electricity for thermal production with HP (MWh)
$vIncDemand_{c,m,h}$ Increase in base demand (MWh)
$vLoadMnew_{m,h}$ New metro consumption curve after changing the base profile (MWh)
$vPowElect$ Contracted annual electric power (MW)
$vPowHP_c$ HP installed capacity (MW)
$vPowPeakM$, $vPowMidpM$, $vPowOffpM$ Contracted annual electric power for the metro system at peak, mid-peak and off-peak hours (MW)
$vPowPV_c$ PV installed capacity (MW)
$vProdPV_{c,m,h}$ Electric PV production (MWh)
$vSOC_{c,m,h}$ Battery State-of-Charge (MWh)
$vSOCEV_{v,m,h}$ EV State-of-Charge (MWh)
$vThBuy_{c,m}$ Thermal energy bought (natural gas) from the grid to meet the daily demand (MWh)

Free variables

$vGridEnTr_{m,h}$ Energy transaction to the grid (MWh)

1. Introduction

The smart city looks for new solutions to many urban challenges (environmental, social and economic) resulting from the interconnection, integrated optimization and operation of systems like transports, waste and energy management, etc., to profit from its potential synergies. However, these synergies are not always evident and should be investigated to obtain the maximum benefit [1].

Fast, efficient and clean mobility and transport systems inside cities are one of the main challenges commonly addressed by local governments, due to the large energy requirements and the significant impact on air pollution and other associated externalities (such as health costs) [2]. With the aim of cleaner and more efficient transport systems, transport regulation measures, such as restricting conventional fuel oil vehicles(CV) transit, are taking place in many cities to reduce pollution [3] and alternatives to conventional transport systems are being investigated and promoted. Among these alternatives, electric vehicles (EV) are one of the most popular and have deserved many research efforts. For example, EV charging strategies have been addressed in Ref. [4], where a review of smart charging systems is presented, the use of EVs as storage has been addressed in Refs. [5] and [6], or its impact on the grid and its use as a tool to foster the introduction of renewable energy in Refs. [7] and [8].

Many approaches to mobility look for increasing efficiency in current transport systems. For example, efficiency on urban rail systems has been object of many efforts and has been commonly addressed in the literature. In this context, a review of energy efficiency solutions has been presented in Ref. [9], identifying five main groups of action: traction efficiency, efficient driving, comfort functions, regenerative braking and smart measurement and management.

From the urban rail systems, the metro (metropolitan trains) is one of the most used. Considering the numerous and frequent stops of the metro trains, regenerative braking can potentially provide important energy savings [10]. To maximize the use of braking energy, three main strategies have been commonly proposed. The first one is the optimal design of the train schedules to synchronize the braking of trains arriving to a station with the departing of other trains within the same electrical sections, allowing accelerating trains to use the braking recovered energy without the need of storage. An example of this solution has been presented in Ref. [11], where a programming problem has been proposed to find an optimal schedule in a real metro system application. The second approach consists in using energy storage systems to store the braking energy. This solution has the benefit of not needing complex train synchronization, maximizing the energy recovery, but has higher costs due to the extra storage infrastructure. The main storage technologies for both on-board and wayside applications have been reviewed in Ref. [10]. Lastly, the third approach consists in using reversible substations able to return the braking energy back to the grid. An example of this solution can be found in Ref. [12].

Table 1 summarizes the research works mentioned above. It can be seen that there are efforts focusing on the integration of EVs and DER systems. However, the connection of public transport systems with urban districts and distributed energy resources has been barely addressed in the literature. In particular, the reviewed metro related works do not include other elements such as EVs of renewable energy sources. Some pilot projects such as [13] have proven possible the connection metro-EV, motivating further research on this and other similar schemes. Hence, one of the main contributions of this paper is the quantitative analysis of the synergies and economic benefits of an interconnected urban environment with distributed energy resources (DER), private electric vehicles and electric public transport (metro). Note that such analysis considering all these systems has not been found in the literature (see the last row in Table 1). Another relevant contribution is the assessment of the impacts of the EV penetration level and the district load size. This analysis provides insight on the potential synergies of these systems, suggesting new possibilities of coordinated management on smart city environments.

A linear programming (LP) problem has been proposed due to its relatively simple modelling and fast solution times. The LP model in-

Table 1
Summary of the reviewed Metro and EV models and research work.

Ref	Methodology	Metro	EV	DER	Focus	Time scope
4	Various		X		Smart charging	short-term
5	MILP		X		Smart charging	short-term
6	MILP		X	X	System operation	short-to-medium-term
7	Analytical		X	X	Integration of renewable sources	short-term
8	MILP		X		Integration of renewable sources	medium-term
9	Analytical	X			Reduction of energy use	med-long-term
10	Analytical	X			Reduction of energy use	med-long-term
11	MILP	X			System operation	short-to-medium-term
12	Simulator	X			Reduction of energy use	med-long-term
This paper	LP	X	X	X	Planning and operation	long-term

cludes a residential district with different energy load curves and DER systems, such as PV panels, air-source heat pumps, stationary batteries and demand response systems. A set of EVs with different daily usage patterns and the regenerative braking and electric energy consumption of metro trains connected to an electrical substation have also been modelled. The district selected is a real Madrilenian district where typical residential load profiles have been considered. Consumption and generation profiles of metro trains have been estimated using average values of real train data [14] and approximated distances and trip times of Madrid's metro. PV production has been calculated using typical solar irradiation values of Madrid and Spanish residential and commercial energy tariffs have been used. The outcomes of the model include the optimal investment planning and operation of the DER systems, according to the metro running patterns and EV usage profiles. Economic benefits in energy and power costs have also been assessed for both the metro substation and the residential district considered. Note that there are more detailed non-linear DER and EV systems models, some including metaheuristic methods as reviewed in Ref. [15], which are commonly used for real-time operation problems. However, in long-term planning models (like the one proposed here), the linear version is commonly preferred as such level of detail is no required [16].

The main contributions of this paper are the two analyses developed: the assessment of the synergies of the systems considered depending on the district size and on the number of EVs and the assessment of the impact of large EV penetration levels, looking for the EV saturation point at which the system does not benefit further with more EV storage. In addition, the effect on DER investments and the share of economic benefits between the participants has been discussed. Indeed, detailed analyses of the potential synergies of such interconnected systems including public transports, EVs, DER systems and facilities have not been previously addressed in the literature, as most models and works only focus on one or two type of systems (see Table 1). It is important to remark that different optimization methodologies could have been used to solve this problem (such as metaheuristic techniques), achieving similar results. However, the approach proposed and the analyses developed provide insight on the synergies among systems and potential challenges and could serve as a starting point for further research.

The rest of the paper is organized as follows. Section 2 provides a brief conceptual description of the optimization model and the full mathematical formulation is presented in Section 3. In Section 4, the input parameters for the model and the case studies are described. Results of these case studies are presented and discussed in Section 5 where a comparison among schemes has been performed. Concluding remarks are summarized in Section 6.

2. Model description

Fig. 1 shows the block diagram of the proposed model. It includes the electrical substation of an electrical section of the metro system. The substation is connected to the grid to supply energy to the trains and to other loads at the stations (illumination, heating and ventilation, etc.) and it is connected to a parking lot where the EVs parked can be used as energy storage for the regenerative braking energy recovered. The parking lot is also connected to a district that implements different DER systems. In Fig. 1, the electric grid has been represented in a red box, the three interconnected systems are the brown boxes and the blue boxes represent loads and/or generators. Black lines show electrical connections and the arrows show the directions of the energy flows.

An optimization model has been proposed (see Fig. 2) to schedule the energy transfers between metro and EVs, the charge/discharge of EVs and the sizing and operation of the DER systems to be implemented in the residential district. The main decision variables (outputs) of the model are:

- DER installed capacity (PV, HP and Battery systems).
- DER operation schedule (PV and HP energy production, Battery charge and discharge schedule, SOC, etc.) according to the available capacity.
- EV operation schedule (charge and discharge schedule, SOC, etc.) according to the available capacity.
- Metro-EV energy transfer schedule, according to the metro energy profiles and EV availability.
- Investment and energy costs.

Note that all these variables are continuous and could take any value, potentially giving an infinite number of solutions (see section 3 for the full mathematical formulation).

The main parameters (inputs) for the model are:

- Metro electrical substation energy profiles (hourly consumption and regenerative braking values).
- EV availability and minimum charge requirement profiles.
- DER prices (investment and operation & maintenance), losses and performance parameters.
- District energy profiles (hourly energy consumption values).

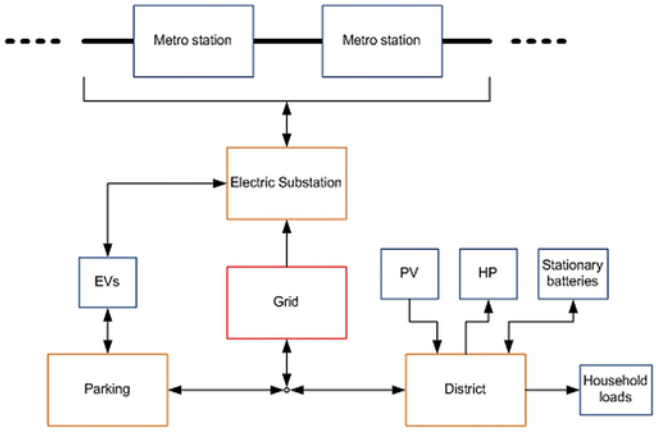

Fig. 1. Block diagram of the proposed system.

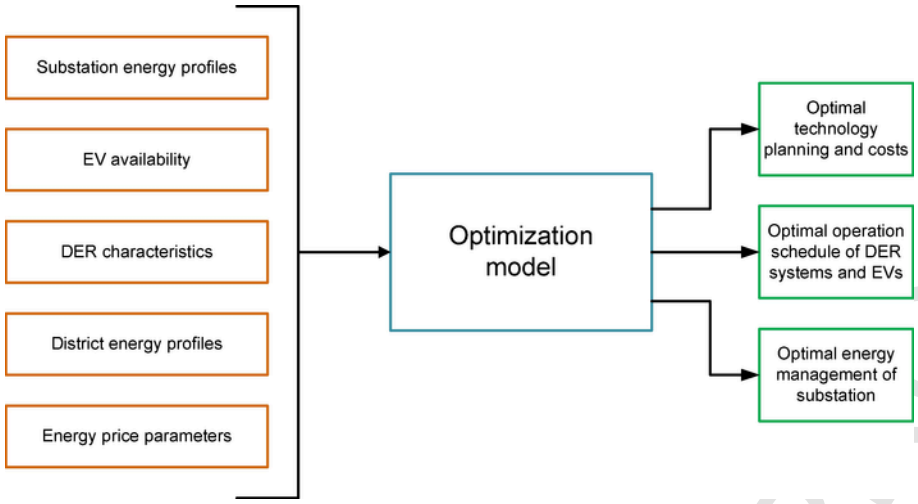

Fig. 2. Optimization model description.

- Energy tariffs.

These parameters are described in detail in section 4.

Note that charging points and interconnection costs have not been considered in this study. Also, it is assumed that these connections are sufficient to implement the analyses developed in this paper. However, given that all systems are already connected to the electric grid, the implementation of the proposed interconnected scheme could be relatively easy, just investing on appropriate network reinforcements and information and communication technologies [17].

3. Mathematical formulation

This section presents the mathematical formulation of the linear optimization model proposed. The model has been implemented in GAMS [18] (a well-known mathematical modelling tool) and CPLEX has been selected as the LP solver, due to its high performance and fast solution times [19]. The model has been run in a standard desktop PC with an Intel i7 processor (running time of less than a 1 min).

3.1. Objective function

The objective function to minimize comprises the costs of all the system considered, including EVs, metro and prosumers (producers-consumers). This formulation considers a total lifespan of 20 years and stationary battery replacements every 8 years [20]. All possible investments take place at the beginning of the study period. A typical year's operation has been replicated for the total length of the study and has been characterized by 12 representative days, each one for a different month of the year [17].

The objective function (1) adds the DER investments and maintenance costs and the net energy costs of all systems.

$$\begin{aligned} min\ \{&costDistEE + costDistPowE \\ &+ costPV + OMPV + costBat + costET \\ &+ costPowT + costHP + OMHP + costDR \\ &+ costMetroEE + costMetroPowE + costEV\} \end{aligned} \tag{1}$$

The terms in (1) are detailed in equations (2)–(14). They include the district net electricity costs due to the energy transactions with the electric grid (2), considering the cost of buying energy (energy * price = *vGridEnBuy* * *pBuyEpriceH*) and the benefit of selling energy back to the grid (*vGridEnSell* * *pSellEpriceH*). Also, the contracted electric power costs (3), the district thermal energy (4) and the thermal power costs (5) as the contracted power tariff per client. They also include the DER investments and maintenance costs (6)–(11), the metro energy (12) and the metro contracted power costs (13), separated in three time-of-use periods: peak, mid-peak and off peak. Lastly, additional EV costs (14) are considered due to the extra batteries degradation produced by the connection with the other systems (see Fig. 1). Indeed, according to EV manufacturers, battery packs should be replaced every 5–8 years [20,21]. For this study, it has been assumed that the extra degradation of the EV batteries due to the additional charge/discharge cycles produced by the metro system will result in an extra battery pack replacement during the study lifespan.

$$\begin{aligned} costDistEE = \sum_{y,m,h} \big(&pCostE_y \\ &* pDaysM_m \\ &* \big(pBuyEpriceH_{m,h} \\ &* vGridEnBuy_{m,h} - pSellEpriceH_{m,h} \\ &* vGridEnSell_{m,h} \big) \big) \end{aligned} \tag{2}$$

$$\begin{aligned} costDistPowE = \sum_{y} \big(&pCostE_y \\ &* pFixEpow \\ &* vPowElect \big) \end{aligned} \tag{3}$$

$$costET = \sum_{y,c,m} \big(pCostT_y * pDaysM_m * vThBuy_{c,m} \big) \tag{4}$$

$$costPowT = pLifespan * 4 * pHouseNum * pFixTpow \quad (5)$$

$$costPV = \sum_{c} \left(pCostPV * vPowPV_{c}\right) \quad (6)$$

$$OMPV = \sum_{C} \left(pOMfixPV * vPowPV_{c} * pLifespan\right) \quad (7)$$

$$costBat = \sum_{c} \left(pCostBat * vBatCap_{c}\right) \quad (8)$$

$$costHP = \sum_{c} \left(pCostHP * vPowHP_{c}\right) \quad (9)$$

$$OMHP = \sum_{C} \left(pOMfixHP * vPowHP_{c} * pLifespan\right) \quad (10)$$

$$costDR = 4 * pHouseNum * pDRequipCost \quad (11)$$

$$costMetroEE = \sum_{y,m,h} \left(pCostE_{y} * pDaysM_{m} * pBuyEpriceM_{m,h} * vLoadMnew_{m,h}\right) \quad (12)$$

$$costMetroPowE = \sum_{y} \left(pCostE_{y} * (pPeakPowM * vPowPeakM + pMidpPowM * vPowMidpM + pOffpPowM * vPowOffpM)\right) \quad (13)$$

$$costEV = pCostBat * pEVnum * pEVcap \quad (14)$$

3.2. Stationary batteries state-of-charge constraints

The state-of-charge (SOC) of a battery is the percentage of stored energy with respect to its maximum capacity, similar to a fuel gauge. These constraints describe the battery storage systems implemented in the district, limiting the energy charge/discharge given the maximum capacity and SOC and computing the current SOC from the previous one, considering the energy charged and discharged and the battery efficiency. It is also considered that the battery starts without any charge at the beginning of the study (15) as if they were just installed, but the following days retain the charge of the previous day (16), (17).

$$vSOC_{c,m=1,h=0} = 0 \quad (15)$$

$$vSOC_{c,m,h=0} = vSOC_{c,m-1,h=24} \ \forall m \in [2, 12] \quad (16)$$

$$vSOC_{c,m,h=1} = vSOC_{c,m,h=24} \ \forall m \in [2, 11] \quad (17)$$

$$vSOC_{c,m,h} \leq vBatCap_{c} \quad (18)$$

$$vSOC_{c,m,h} = vSOC_{c,m,h-1} + \left(vChBat_{c,m,h} - vDisBat_{c,m,h}\right) / pEffBat \quad (19)$$

$$vDisBat_{c,m,h} \leq vSOC_{c,m,h-1} \quad (20)$$

$$vChBat_{c,m,h} \leq vBatCap_{c} - vSOC_{c,m,h-1} \quad (21)$$

3.3. Demand response constraints

Constraints (22) and (23) model the load shifting considered for the proposed demand response scheme. From the original load, a maximum amount of load shifting per day has been set by the *pDemandShift* parameter as a percentage of the original daily energy consumed (24). Constraint (25) is used to force a baseload that cannot be shifted in time (i.e. the energy equivalent of a fridge which is approximately 100 W per house [22]).

$$\sum_{h} vDemandNew_{c,m,h} = \sum_{h} pDemandElec_{c,m,h} \quad (22)$$

$$vDemandNew_{c,m,h} = pDemandElec_{c,m,h} + vIncDemand_{c,m,h} - vDecDemand_{c,m,h} \quad (23)$$

$$\sum_{h} vIncDemand_{c,m,h} \leq pDemandShift * \sum_{h} pDemandElec_{c,m,h} \quad (24)$$

$$vDemandNew_{c,m,h} \geq 0.0001 * pHouseNum \quad (25)$$

3.4. Energy production constraints

These constraints model the production of the PV and HP systems. In (26) (taken from Ref. [23]), GHI stands for global horizontal irradiance (W/m2), which is the energy provided by the sun at a specified location, *vPowPV* refers to the installed capacity of the PV sys-

tem and G is the theoretical maximum global irradiation received on a horizontal plane (G = 1000 W/m2) which provides the maximum generation value (at 100% efficiency) used by fabricants as a base line to define the maximum peak power of a PV system. Equation (27) relates to the thermal production by the air-source heat pump. The thermal generation is considered to have a greater output than its actual production as it is compared with the cost of producing the same amount of energy with a conventional gas boiler (80% efficiency).

$$vProdPV_{c,m,h} = \frac{pGHI_{m,h} * vPowPV_c}{G} * (1 - pLossesPV) \quad (26)$$

$$vThBuy_{c,m} = pDemandTherm_{c,m} - \sum_h \left(vHPenInput_{c,m,h} * pCOP * (1 - pLossesHP)\right) / 0.8 \quad (27)$$

Constraint (28) has been used to limit the thermal production of the heat pump below the nominal installed electric input power and (29) has been implemented to produce at least 30% of total demand in the afternoon-evening hours. This has been made to avoid having the thermal generation only in hours where it is less likely to be used.

$$vHPenInput_{c,m,h} \leq vPowerHP_c \quad (28)$$

$$\sum_h \left(vHPenInput_{c,m,h} * pCOP\right) * \frac{(1 - pLossesHP)}{0.8} \geq 0.3 * pDemandTherm_{c,m} \; \forall h \in [13, 20] \quad (29)$$

Equation (30) has been used to calculate the required contracted electric power in the district given the DG production and loads.

$$vPowElect \geq vGridEnBuy_{m,h} \quad (30)$$

3.5. Balance equation

The total energy consumption and production is balanced with (31). In this equation, all energy entering the node is positive and the energy leaving the node is negative. Equation (32) separates the energy transactions with the grid in its positive and negative parts to use the appropriate tariffs to sell and buy energy.

$$vGridEnTr_{m,h} = \sum_c \left(vDemandNew_{c,m,h} - vProdPV_{c,m,h} - vDisBat_{c,m,h} + vChBat_{c,m,h} + vHPenInput_{c,m,h}\right) + \sum_v \left(-vDisEV_{v,m,h} + vChEV_{v,m,h}\right) \quad (31)$$

$$vGridEnTr_{m,h} = vGridEnBuy_{m,h} - vGridEnSell_{m,h} \quad (32)$$

3.6. EVs state-of-charge constraints

Similar to the stationary battery SOC constraints, the EVs have a set of constraints that govern their behaviour. The main differences in comparison to the abovementioned constrains are in (36) and (37), where the EV storage capacity (available capacity) changes over time and for each type of EV user. Also, there is a minimum SOC requirement. Furthermore, EVs can arrive to the parking lot with a pre-existing charge (39). These parameters represent the usage profiles of the EV drivers.

$$vSOCEV_{v,m=1,h=0} = pSOCminEV_{v,h=1} * pEVnum \quad (33)$$

$$vSOCEV_{v,m,h=0} = vSOCEV_{v,m-1,h=24} \; \forall m \in [2, 12] \quad (34)$$

$$vSOCEV_{v,m,h=1} = vSOCEV_{v,m,h=24} \; \forall m \in [2, 11] \quad (35)$$

$$vSOCEV_{v,m,h} \leq pAvailEV_{v,h} * pEVnum \quad (36)$$

$$vSOCEV_{v,m,h} \geq pSOCminEV_{v,h} * pEVnum \quad (37)$$

$$vDisEV_{c,m,h} \leq vSOCEV_{c,m,h-1} \quad (38)$$

$$vSOCEV_{v,m,h} = vSOCEV_{v,m,h-1} + \left(vChEV_{v,m,h} - vDisEV_{v,m,h}\right) / pEffBat + pSOCinitEV_{v,h} * pEVnum - vDisMetro_{v,m,h} + vChMetro_{v,m,h} \quad (39)$$

3.7. Metro constraints

Metro constraints limit the EV energy charge from the available regenerative braking energy (40) and compute the new electric load curve of the electrical substation, changed from the original by the energy coming from EVs (41). Equations (42)–(46) compute the Metro contracted power at peak, mid-peak and off-peak tariff periods. These periods are defined with the month m and hour h subsets: mS, mW, hO, hMs, hMw, hPs and hPw.

$$\sum_{v} vChMetro_{v,m,h} \leq pMetReg_{h} \quad (40)$$

$$vLoadMnew_{m,h} = pMetLoad_{h} - \sum_{v} vDisMetro_{v,m,h} \quad (41)$$

$$vPowOffpM \geq vLoadMnew_{m,hO} \quad (42)$$

$$vPowMidpM \geq vLoadMnew_{mS,hMs} \quad (43)$$

$$vPowMidpM \geq vLoadMnew_{mW,hMw} \quad (44)$$

$$vPowPeakM \geq vLoadMnew_{mS,hPs} \quad (45)$$

$$vPowPeakM \geq vLoadMnew_{mW,hPw} \quad (46)$$

4. Case study description and parameters

Several case studies have been proposed to analyse the impacts of EV penetration. The case studies estimate Metro de Madrid energy usage data and simulate the consumer behaviour of Villaverde district in southern Madrid. It has been assumed that the buildings of the district under study do not have any pre-existing DER installation. The input parameters considered in this study are described next, following the same order shown in Fig. 2.

4.1. Substation energy profiles

Line 3 of Metro de Madrid was selected for this study due to its high passenger load [24]. It has 18 metro stations served by 6 electrical substations [11,25]. Since substation's exact location is not publicly available, it was assumed that they are uniformly located throughout the metro line, i.e. one substation every three to four metro stations. In this study, a section of metro line 3 (starting from Villaverde Alto to Ciudad de los Ángeles stations, see Fig. 3 taken from Ref. [26]) was selected due to its proximity to residential districts and public parking lots, assuming that one substation at the beginning of metro line 3 serves energy to Villaverde Alto, San Cristóbal, Villaverde Bajo-Cruce and partly to Ciudad de los Ángeles stations, where a second substation is likely to be located.

Using the metro line 3 interstation distances (estimated with google maps, [27]) and trip times (taken from current metro schedules, [26, p. 3]) and considering the average energy consumption per distance and per trip time values proposed in Ref. [14], the train traction energy has been calculated for the selected section of metro line 3. The regenerative braking energy has been computed considering that only 1/3 of the train traction energy can be reused [10] and the total electric load of the train has been calculated by adding 20% of traction energy for the non-traction loads [10] (station loads, ventilation, etc).

Table 2 shows the energy usage and regenerated braking energy obtained by the trains operating between Villaverde Alto and Ciudad de los Ángeles stations (including the non-traction energy). It has been considered that the same energy is required in both directions. Moreover, catenary lines of the trains are normally connected to two electrical substations and the energy to feed the train can come from both. Unfortunately, since detailed information on tracks and electrical connections is not available, it has been considered that the energy required by the trains is equally shared between the two substations.

It is important to remark that the usable regenerated energy can be used for different purposes. For instance, it can be used when possible to supply departing trains or for other non-traction loads both in the trains and stations. According to the analysis developed in Ref. [28], it has been considered that from all the usable energy 43% goes to other trains and station loads, 50% to the external EV systems and 7% to additional electrical losses.

Metro systems are normally scheduled either following a timetable or in time intervals (a train passes through a station every certain amount of time). Metro de Madrid implements time intervals, whose length depends on the day of the week and the hour. Considering the average time intervals of metro line 3 during a standard weekday (Monday to Thursday) provided in [26], p. 3], Fig. 4 shows the computed energy profiles for the selected electrical substation, taking into account the energy values of Table 2 and the number of trains trips per hour, according to the service frequency previously discussed. Also, taking into account the considerations of the regenerated energy distribution mentioned before (part of the regenerated energy goes to the EVs and part goes to other trains, reducing the net energy consumption).

Fig. 3. Station plan of Madrid's metro line 3.

Table 2
Consumed and regenerated energy per train and journey, between the Villaverde Alto and C. de los Angeles metro stations.

	Traction	Non-traction	Total
Consumed energy (kWh)	45	9	54
Regenerated energy (kWh)	15	–	15

4.2. EV availability

Villaverde district has 5 public parking lots for residents [29]. Among them, San Aureliano was selected as the parking lot for EVs due to its relatively large capacity (194 parking spots) and its proximity to the electrical substation chosen for this study.

A normal practice in Madrilenian residential neighbourhoods during the week days is that the residents leave to work in the morning, around 6h00 – 8h00 and come back home around 17h00 – 19h00. It is also common that many people living in suburbs away of the city centre arrive in their cars to parking lots close to metro or commuter train stations, occupying the residents' empty places and continue their journey in public transport systems. Therefore, both district residents and visitors EV users have been modelled (see Fig. 5). Residents' EVs are fully available as storage systems until 5h00 when they start to move to work, causing a slow decrease in EV storage availability. Conversely, the visitors start to arrive to the parking lot at 6h00 and leave from 16h00, liberating the places for the residents. Following the recommendations given by most manufacturers to extend battery life [30], it has been established a minimum SOC of 20% at all times the car is parked and, complying with the requirement of EV users, a minimum SOC of 80% has been set for the time the car leaves the parking lot. It has been also considered that the EV arrives to the parking lot with a SOC level of 40% (i.e. the energy required for the journey is 40% of the total EV capacity, approximately 50 km) [31,32]. It has been considered that the total storage capacity of each EV is 19 kWh [33].

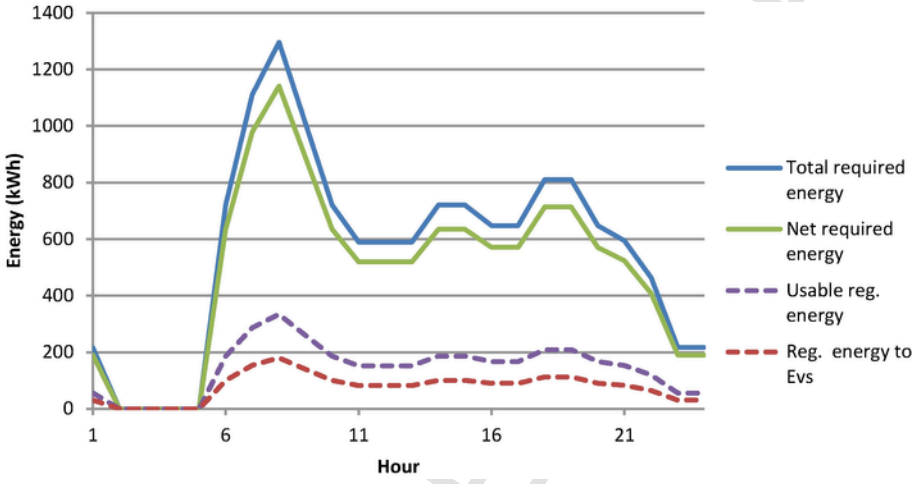

Fig. 4. Villaverde Alto substation energy profiles.

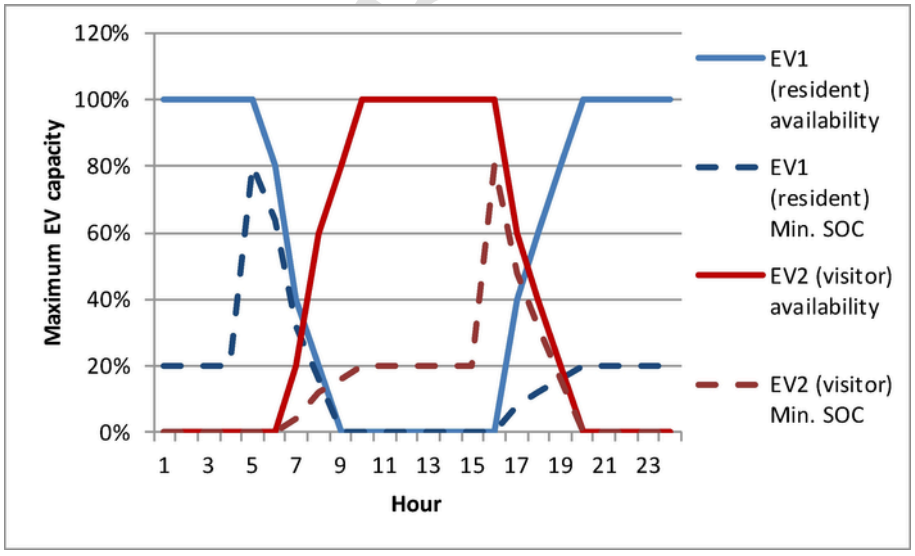

Fig. 5. EV user availability and minimum State-of-charge requirement.

4.3. DER characteristics

The distributed energy resources considered for the district (apart from the EV) are photovoltaic (PV) panels, air-source heat pump (HP), stationary batteries and demand response systems. The solar production from the PV has been calculated with average hourly solar global horizontal irradiance data for Madrid, at 35° inclination and facing south (taken from Ref. [23]). Table 3 lists the costs and performance parameters of the considered DER, taken from Ref. [17]. The coefficient of performance (COP) of the heat pump has been assumed in 2.5 units, while the *pDemandShift* parameter has been calculated considering the appliances that can be more easily shifted in time. According to [34], the washing machine, dryer and dish washer represent the 13.3% of the total electric consumption of a typical Spanish household; hence, the *pDemandShift* has been set to a maximum of 13% of total daily load. Also, a minimum baseload is stablished with equation (25). The *pDRequipCost* parameter, representing the cost of the control devices needed for demand response has been set to 250 €/house [35].

4.4. District energy profiles

Expected household energy profiles are required to adequately plan and operate the DER systems and their integration with the metro substation. Reference [36] classifies Spanish residential customers in 4 types according to the age of the head of the family (HF) and the presence of children in the household (younger than 12 years). The total annual energy consumption also differs among client types. Table 4 summarizes the energy consumption per client type and the difference with respect to the Spanish average values.

In this paper, the monthly demand variation throughout the year [36] and the typical electricity demand curves for each type of client have been used (these energy profiles can be found in Ref. [37]). It has been assumed that the users follow the same changes in percentage of total consumption in thermal and electric energy.

4.5. Energy price parameters

A time-of-use tariff was used for the households' electricity consumption including EV charging, while thermal energy was priced with a static tariff. Table 5 presents the energy tariffs selected (from Refs. [38,39]). It has been assumed that the prosumer can sell electricity back to the grid at a fixed price of 0.0421 €/kWh, ignoring the network costs and the time discrimination. In other words, this sell price is calculated considering that approximately 40% of the electricity tariff correspond to energy costs and the rest goes to taxes and network costs [40], so the assumed sell price corresponds only to the value of the energy sold and not to network costs or taxes.

Detailed information of Metro de Madrid energy transactions is not publicly available. However, reference [41] shows an example of a contract between Metro de Madrid and two Spanish retailers buying electric energy at prices ranging from 0.08 to 0.10 €/kWh. Therefore, it seems sensible to consider that the metro has a commercial high voltage tariff, like the one presented in Ref. [42], with a time-of-use discrimination for both energy and power and different time schedules for winter and summer months. Table 6 summarizes the selected tariff values for the metro system.

4.6. Case studies description

For the sake of clarity, the case studies have been labelled with the abbreviation **CS** for Case Study, a sub-index that refers to the number of houses per house type considered in the district and a second sub-index with two letters that refers to the selected options. Upper case **D** stands for DER systems installation, while lower case **d** stands for no DER systems installation and upper case **C** stands for the energy unconstrained metro-EV connection while lower case **c** stands for the constrained metro-EV installation. Note that these options imply different model alternatives as seen in section 2. For instance, $\mathbf{CS_{500DC}}$ refers to the full model described in section 2, with a district size of 500 × 4 houses (i.e. 500 houses per household type) implementing DER and with complete connection metro-EV (no limiting the energy transfers), while $\mathbf{CS_{250dC}}$ correspond to 250 × 4 houses without DER implementation but with full metro-EV connection. Table 7 summarizes the three model variants considered in this paper.

The case studies proposed in this paper and developed in the following subsections have two main objectives:

Table 3
Technology costs and expected energy losses.

Technology	Inst. Cost (€/W)	O&Mfix (€/kW)	Losses (%)
PV	2.15	30.93	24 (electric)
HP (COP = 2.5)	2.94	100.1	15 (thermal)
Battery	0.36 (€/Wh)	–	10 (electric)

Table 4
Total annual energy consumption per client type.

Type of client	Comparison to average	Annual Thermal (kWh)	Annual Electric (kWh)
1	−5%	6054.9747	3507.0613
2	8%	6871.7046	3980.1140
3	−19%	5174.3962	2997.0274
4	16%	7422.3987	4299.0778

Table 5
Residential energy tariffs and time schedules.

	Peak	Mid-peak	Off-peak
Electric energy (€/kWh)	0.1632	0.0843	0.0564
Electric Power (€/kW)		49.28617	
Time schedule	13-23 h	7-13, 23-1 h	1-7 h
Natural gas variable (€/kWh)		0.0568	
Natural gas fixed (€/year)		52.32	

Table 6
Metro energy tariffs and time schedules.

	Peak	Mid-peak	Off-peak
Energy (€/kWh)	0.126623	0.109203	0.080358
Power (€/kW)	59.47529	36.67681	8.410411
Schedule winter	17-23 h	8-17 h & 23 h	0-8 h
Schedule summer	10-16 h	8-10 h & 16-0 h	0-8 h

Table 7
Summary of case studies considered.

Case study	Description
CS_{DC}	DER systems implemented and free connection metro-EV
CS_{dC}	DER systems NOT implemented, but with free connection metro-EV
CS_{Dc}	DER systems implemented, but with limited metro-EV power flow (the metro cannot receive more energy than sent to the EVs each day)

- to analyse the effect of the number of available EVs within the selected parking lot and of the size of the district on the DER investment decisions and the total district energy costs,
- to find the saturation level where the system does not benefit further from more EV storage.

5. Results and discussion

5.1. Analysis of the effect of EV penetration and district size

According to [43], there are 43109 inhabitants in San Andrés neighbourhood of Villaverde. For this first objective, three scenarios have been considered corresponding to three district sizes, assuming that only a partial share of the inhabitants chose to participate in DER installation (but fully implementing DER systems with unrestricted metro-EV connection, corresponding to sub-indexes **DC**). Following the 4 types of households described in section 4.4, the three case studies are: 4 house types x 250 houses per type, 4 × 500 and 4 × 1000 (which are possible to fit in the Villaverde district). For these three district sizes, different numbers of EVs going from 25 to 194 EVs have been considered, 194 being the maximum capacity of the selected parking lot. For all cases optimal DER investments are determined by minimizing the total system costs including DER investment costs and the operating costs of metro, districts and EV as defined in (1).

The resulting installed capacity of DER systems for the three district sizes has been depicted in Fig. 6. By analysing the results, the following considerations can be made.

- The investments in the DER systems considered increase almost linearly with the district size: for instance, $\mathbf{CS_{500DC}}$ installs around 60% more PV systems than $\mathbf{CS_{250DC}}$ and $\mathbf{CS_{1000DC}}$ about 70% more than $\mathbf{CS_{500DC}}$. In addition, this PV increment is almost independent of the number of EVs. This is due to the fact that, in this study, the PV system is an important supplier of electricity for the district and the EV electric demand is very small in comparison with the household electricity demand. Hence, the consumption increase due to the EV is not very significant with respect to the total district consumption and therefore with respect to relative additional PV generation needed. Note, as shown in Fig. 4, that the metro load is larger than the EV load and has a profile that takes advantage of the sunny hours, increasing the amount of PV capacity to install. However, when the district load becomes large enough (in relation with the metro and EV loads), the PV capacity increases almost linearly with the district size.
- The heat pump investments are barely affected by the EV numbers. Indeed, the change is negligible, less than 1% and is due the small change in PV production for the extra EV electric load, something expected, since EV load is purely electric and does need any thermal production from the HP system.
- Battery systems investments depend on both, the district size and the number of EVs. Larger districts profit from more battery installation, but larger amount of EVs provides "free" storage capacity decreasing batteries investments needs. The rate of substitution of battery by EV storage is around 60% (for each kWh of extra EV storage, the battery system decreases its capacity in 0.6 kWh), which is a measure of the available extra storage that EVs are able to provide to the district, conditioned by their availability constraints (see Fig. 5). Different EV availability profiles are likely to produce different substitution ratios.

The average annual electric power and energy costs for the metro are shown in Fig. 7. With larger number of EV, the additional EV storage can be used by the metro which then reduces significantly its costs, especially for $\mathbf{CS_{250DC}}$, where the savings in energy and power costs can go up to 25% comparing the case of 25 EVs with 194 EVs. Conversely, $\mathbf{CS_{1000DC}}$ shows a smaller benefit of 15% for power and 9% for energy costs (from 25 to 194 EVs). In these scenarios with larger districts sizes, the higher energy requirements of the households represent a larger cost than the metro in the objective function, so the cost minimization delivers more EV storage capacity to the district (to store PV energy and provide load shifting), leaving less capacity for the metro.

The average annual electric power and energy costs for the district, including EVs consumption, are shown in Fig. 8. The electricity costs increase slightly with EVs due to the additional EV energy re-

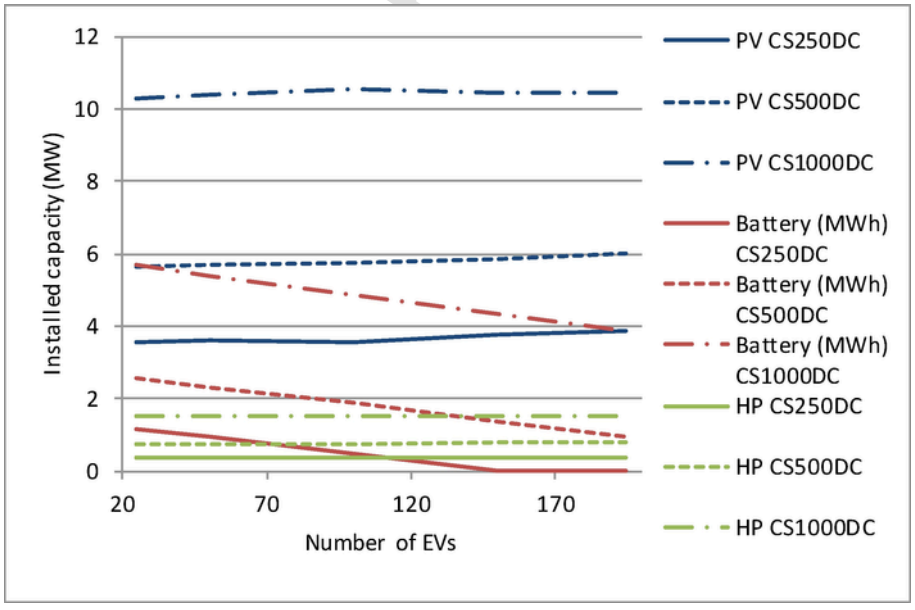

Fig. 6. Installed capacity of DER systems for different district sizes and with full connection metro-EV.

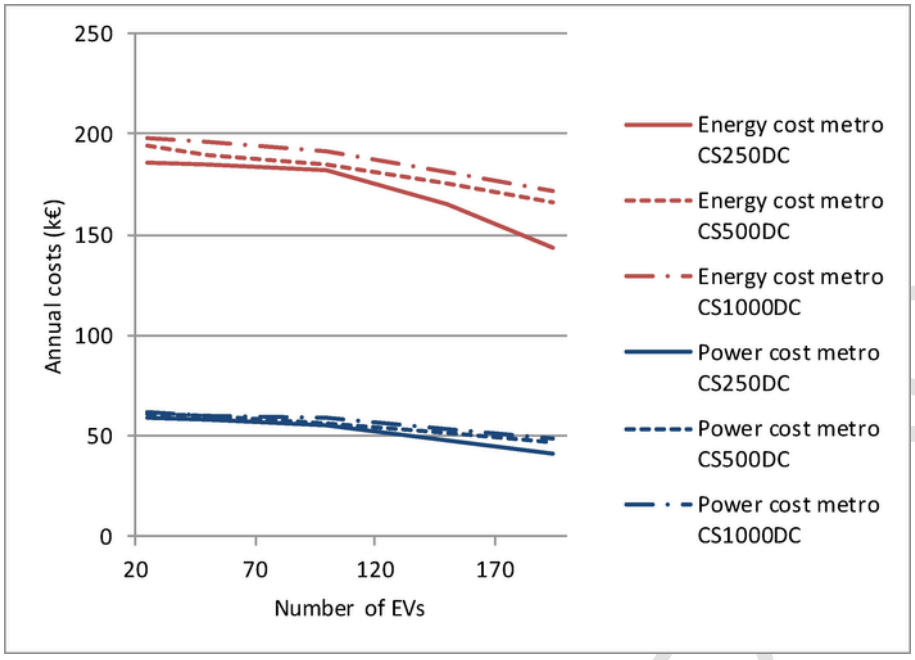

Fig. 7. Annual electric energy and power costs for the metro substation.

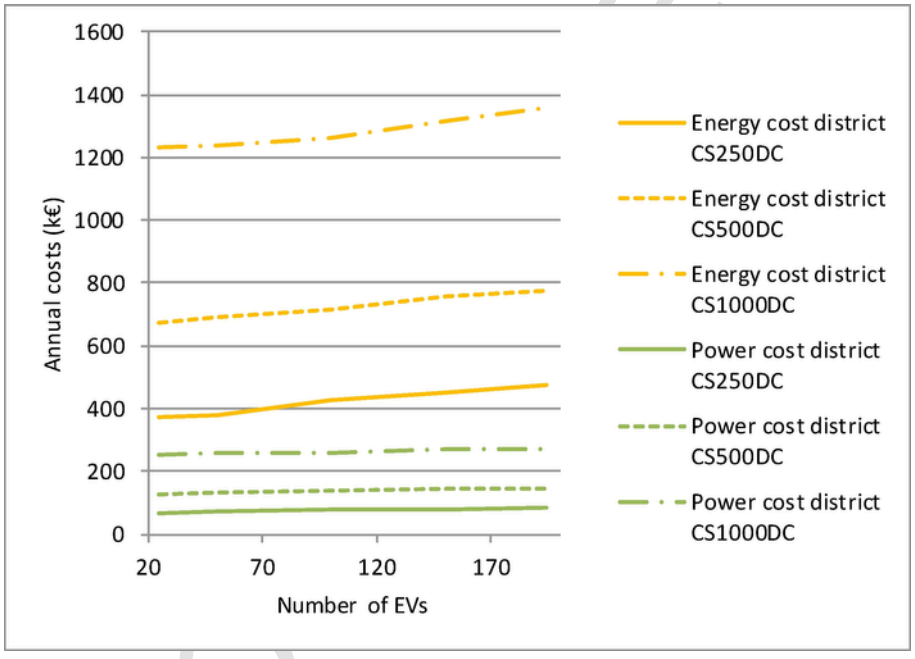

Fig. 8. Total annual energy and power costs for the district.

quirements (increment of 11–19%, or 1.5–3 million euros for the whole 20-year period), which is approximately 743€ per extra EV and per year in $\mathbf{CS_{1000DC}}$ (note that and independent not connected EV would costs approx. 775€ per year). Looking at the total costs (including metro, district, DER and EV costs, see Fig. 9), a similar increment can be seen.

However, if EVs charging and EV battery replacement costs are removed, since EVs deployment respond to other objectives and requirements, it is possible to see more clearly the effect of the synergies provided by both the extra storage and the interconnectivity of systems. As can be seen in Fig. 9, the savings in total costs (without including EV costs) are around 2–5%. Comparing this savings to those of the metro system (up to 25% in $\mathbf{CS_{250DC}}$), it is possible to see that the metro benefits considerably more from EVs than the district (see Fig. 7). This is caused by the fact that the overall costs are minimized when the metro uses the EV energy charged with the PV production and the cheaper off-peak energy from the district (which is a smaller share of the overall costs at those hours).

Table 8 summarizes all the results shown in this section, taking the three case studies with the smaller number of EVs (25 vehicles)

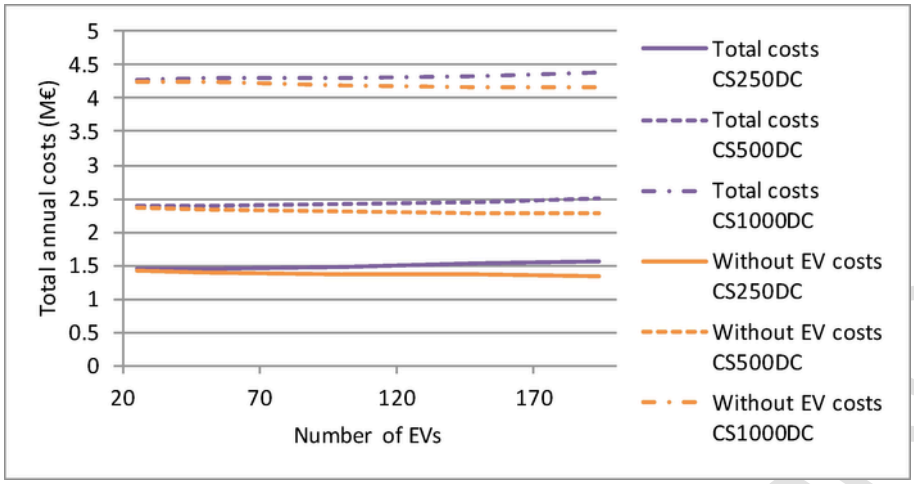

Fig. 9. Total annual costs for all the considered systems including DER investments and without EV costs.

Table 8
Summary of capacity and costs increments when the EV number goes from 25 to 194.

	CS_{250DC}	CS_{500DC}	CS_{1000DC}
PV	10%	6%	2%
HP	1%	1%	0%
Battery	−100%	−64%	−32%
Metro costs	−25%	−17%	−15%
District costs	27%	15%	10%
Total costs (without EV costs)	−5%	−3%	−2%

and comparing them with the scenario of 194 EVs, showing the changes in DER capacity and costs increments. Once again, it can be seen that the PV and HP systems are not significantly affected by the EV penetration, while the battery capacity is heavily impacted. Also, the metro cost reductions are more affected by the number of EVs than the district (especially in $\mathbf{CS_{250DC}}$), as the metro system uses more the EV storage because it represents a larger share from the total costs.

5.2. System saturation due to EV penetration

For the second objective, the three cases $\mathbf{CS_{250dC}}$, $\mathbf{CS_{250DC}}$ and $\mathbf{CS_{250Dc}}$ have been considered. The first one does not implement DER systems and does not limit the metro-EV connection, the second one implements DER systems and does not limit the metro-EV connection (to analyse how the metro system profits from the DER systems placed in the district, taking extra energy from the district via the EVs) and the third one implements DER systems but limits the metro-EV connection (so the metro can only take from the EVs the same amount of energy stored from the regenerative braking), limiting the energy transfers between metro and EVs according to (47). In all cases the district size remains constant (1000 houses), but the number of EVs goes up to 5000 vehicles to analyse the implications of larger EV penetration level and to determine the EV saturation point at which the system does not benefit further from more EV storage.

$$\sum_{v,m,h} vDisMetro_{v,m,h} \leq \sum_{v,m,h} vChMetro_{v,m,h} \tag{47}$$

Looking at the metro energy costs (Fig. 10) and the energy transfers between the EV and the metro electrical substation (Fig. 11), the first results that stands out is that for $\mathbf{CS_{250Dc}}$, with the metro-EV energy transfer limited (energy flows from metro to EVs and the converse are both equal), the resulting costs are barely affected by the number of EVs and are considerably higher than those of the other cases. On the contrary, when the energy from the batteries to the metro is not limited, a much larger cost reduction takes place (see Fig. 10). Indeed, $\mathbf{CS_{250dC}}$ and $\mathbf{CS_{250DC}}$ present an important energy cost decrement (around 97% and 92%, respectively) in comparison with the case of 25 EVs, achieving a similar minimum cost value. This shows that, when it is allowed, more energy comes from the EVs to the metro system than the other way around, so the metro benefits largely from the free storage provided by the EVs. However, $\mathbf{CS_{250DC}}$ and $\mathbf{CS_{250dC}}$ have significantly different EV saturation number and, for instance, with 300 EVs the metro energy costs in $\mathbf{CS_{250dC}}$ is 15 times larger than in $\mathbf{CS_{250DC}}$ (see Fig. 10).

Indeed, when DER investments are allowed, the saturation point is much lower, around 300 EVs, since cheap energy comes also from the installed DER. On the contrary, when no DER is allowed, even if the final costs are similar, the saturation point is much larger, around 2000 EVs, since more storage is needed for the metro to profit from the cheap off-peak energy bought by the district from the grid (this is also shown in Fig. 13, where the detailed operation of the systems is further analysed).

It should be noted that the benefits for the metro system do not increase anymore when the energy transfers metro-EV stop increasing, corresponding to the saturation point. This can be seen in Fig. 11, which shows the energy that goes from the EV to the metro and vice versa for the three case studies. Indeed, for $\mathbf{CS_{250DC}}$ with more than 300 EVs, the metro system receives a constant annual energy flow of around 4050 MWh (this energy transfer could be possible as it corresponds to 11.1 MWh per day, which represent approximately 1 full discharge per EV in the 300 EVs case). A similar behaviour can be seen in $\mathbf{CS_{250dC}}$, but needing 2000 EVs to stabilize (see Fig. 11, EV2Metro_CS250 dC). Note that in Fig. 11, the energy flow from the metro to the EVs is constant to all three case studies, corresponding to the regenerative braking energy available (i.e. all three blue lines and the red one of $\mathbf{CS_{250Dc}}$ are superimposed). Finally, it can be seen that, as expected, the energy going to the electrical substation is considerably larger than the energy sent to the EV parking lot, recovered from regenerative breaking (up to 6.2 times more), which means that the metro system profits from the DER generation and the cheaper energy bought from the grid at the off-peak time residential tariff (paid by the district).

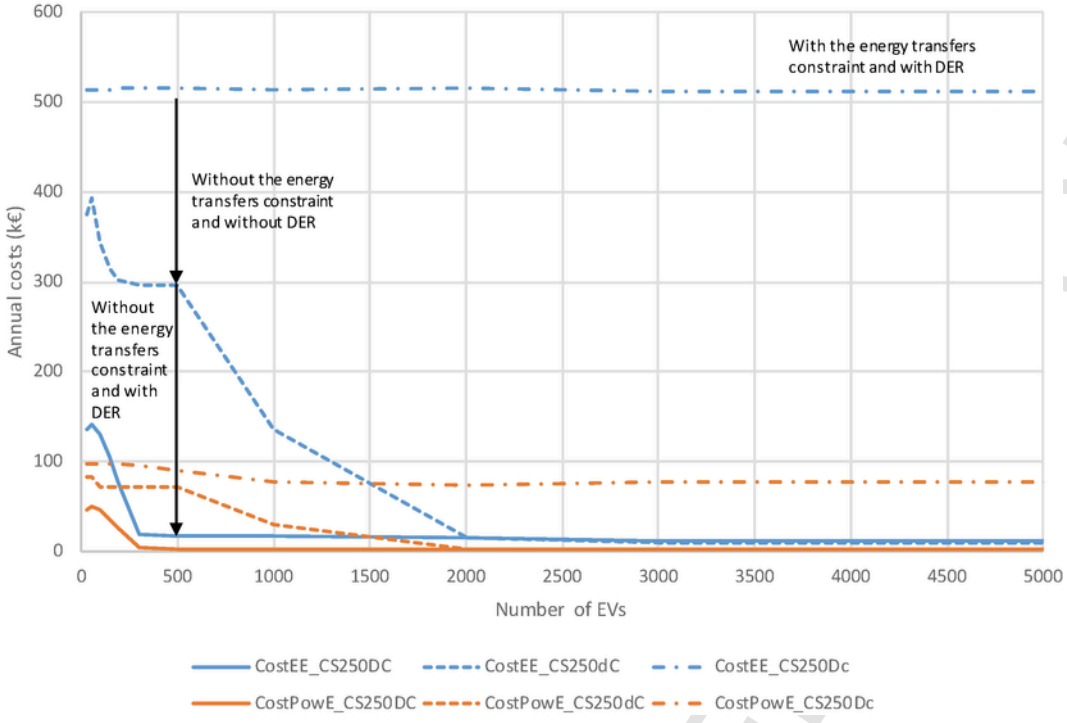

Fig. 10. Annual metro electricity costs for CS_{250DC}, CS_{250dC} and CS_{250Dc} and different levels of EV penetration.

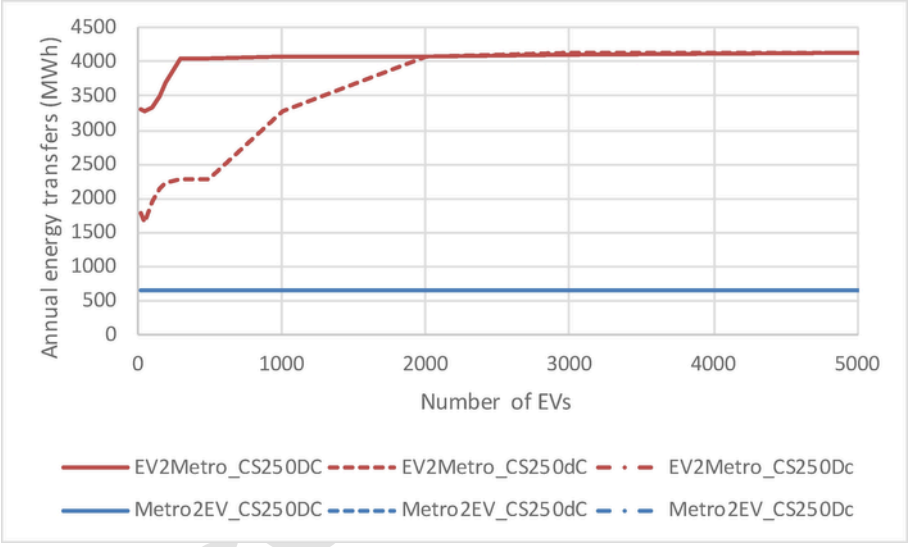

Fig. 11. Annual energy transfers Metro-EV for CS_{250DC}, CS_{250dC} and CS_{250Dc} and different levels of EV penetration.

Table 9 summarizes the effects on the three case studies at their EV saturation point in comparison with the 25 EVs case. Note that the metro energy costs reduction in the cases without the energy flow constraint can go over 90%, while the case with limited energy flows the cost reduction is almost zero. Note also that, the presence of DER systems have a significant impact on the required number of EVs to achieve the maximum cost reduction.

The total annual overall costs, just like the metro system costs, present an EV saturation point when no extra benefit is achieved. This is shown in Fig. 12 (zoomed to 0–1000 EVs since all the saturation points of the considered case studies fall around 200–300 EVs), where the base EV energy charge costs have been removed (the original costs of charging the EV to meet the energy requirements of Fig. 5). For instance, **CS_{250DC}** achieve a minimum total cost with 300 EVs, corresponding to the saturation point of the metro in the same case study (see Fig. 11). For **CS_{250Dc}** the saturation point is around 100–150 EVs, showing that if the energy transfers to the metro are limited, less EV storage is used by the metro and more capacity becomes available to the district for a same number of EVs. Lastly, without DER systems in **CS_{250dC}**, the storage capacity provided by EVs is less used and the saturation point is reached around 100 EVs. This contrasts with the saturation point for the metro system in the same case study (2000 EVs, see Fig. 11). In other words, the district can only shift a certain amount of load (and store PV en-

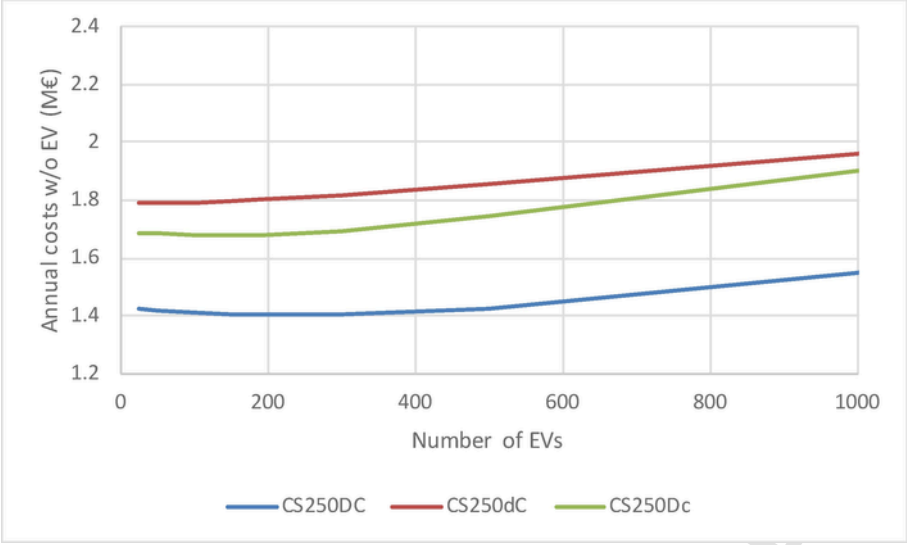

Fig. 12. Annual total costs for different levels of EV penetration (without EV costs).

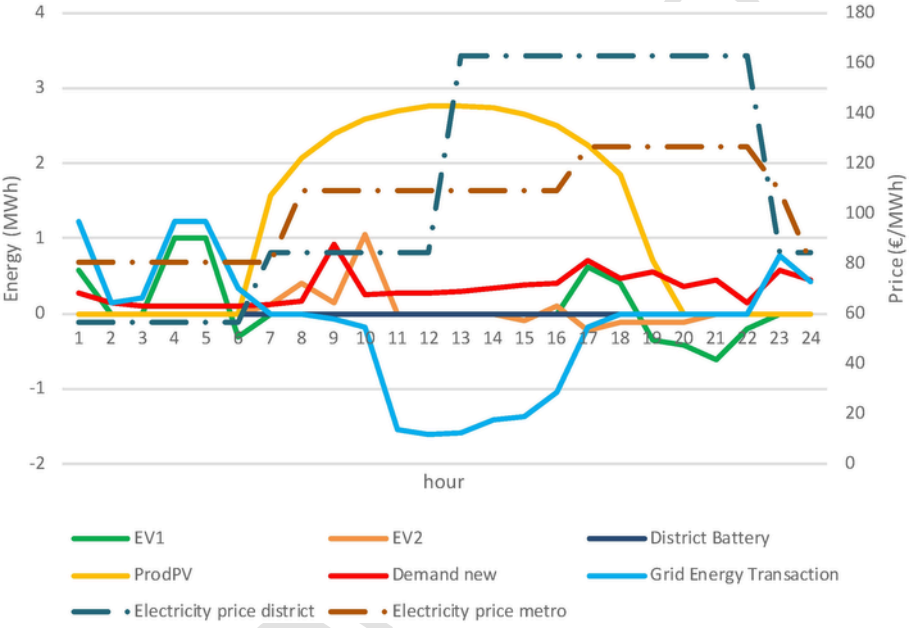

Fig. 13. Operation of the district loads and DER systems for CS_{250DC} and 150 EVs in a summer day.

Table 9
Impacts on the three case studies comparing the 25 EVs case with the EV saturation point.

	CS_{250DC}	CS_{250dC}	CS_{250Dc}
Energy cost savings	89%	94%	0.1%
Saturation point (EVs)	300	2000	25
EV2Metro transfers ratio	6.2	6.2	1

ergy if available) using EV storage. Then, even if more storage capacity is available, the district does not take advantage of it anymore. However, the metro system can still use the discharged energy coming from the EVs.

As discussed before, the metro benefits largely from the DER systems implemented in the district and the energy transfers metro-EV are not the same to the transfers EV-metro (see Fig. 11). Fig. 13 demonstrates it further, looking at the hourly operation of the district and the two types of EV users (labelled as *EV1* and *EV2,* see Fig. 13) in a typical summer day (July) in the **CS_{250DC}**, where energy from the grid (*Grid Energy Transaction,* see Fig. 13) is used to charge the EVs during the early hours with no solar production (labelled as *ProdPV,* see Fig. 13), to be discharged to the metro from 6h00–8h00. Then, when the solar production is large enough it is used to charge the EVs. Note that the majority of the EV capacity is discharged to the metro and only a small part is used to meet the district demand (labelled as *Demand new,* see Fig. 13), which coincides with the time when the price of residential energy is more expensive than the metro commercial tariff. It can also be noted note that there is at least one of the EV types available most of the time, making it less likely to use

the more expensive battery systems if there is enough EV storage capacity.

To conclude this analysis, the total system costs of the three case studies reviewed in this section have been compared to the total costs of a disconnected base case (i.e. all the systems operate independently without any DER implementation or metro-EV connection). Table 10 show the percentage of savings of the case studies. It can be noted that the DER systems produce the higher overall benefits. In the case with DER systems and the energy transfer constraint $\mathbf{CS_{250Dc}}$, the benefits are logically lower than those obtained when DER systems are installed with no energy transfer limits, $\mathbf{CS_{250DC}}$ (average savings of 28–11% vs 15–9%, see Table 10), but they still are considerably higher than the no-DER scenario ($\mathbf{CS_{250dC}}$, savings of 9–5%, see Table 10).

It is also important to remark that the percentage of cost reduction decreases with the number of EVs, due to the saturation points shown in Fig. 12, where extra EVs do not provide useful additional storage capacity but an additional energy consumption that becomes more significant in comparison with the district and metro loads.

5.3. Sensitivity analysis and result discussion

The potential applicability of the results in other contexts has been assessed with a sensitivity analysis on some of the main model parameters. This sensitivity analysis consists in increasing or decreasing by 20% the district and metro energy prices (shown in Tables 5 and 6) and the metro energy profiles (shown in Fig. 4). Table 11 summarizes the total costs of the base case in $\mathbf{CS_{dcL}}$ and the in $\mathbf{CS_{DCL}}$ case for the different value changes. The table shows that the change in benefits is relatively small for all the considered parameters, with benefits in the range of 24%–32% in the studied sensitivity range. This is approx. ±4% variation relative to the original benefits. Therefore, these results suggest that other systems in a similar setup are likely to present comparable synergies as the ones reported in this paper.

Note that a considerable part of these benefits is produced by "opportunistic" synergies, caused by the different tariffs considered (commercial and residential). The metro system with higher commercial tariffs is taking advantage of the cheaper energy coming from the EVs and the district (that uses a lower tariff). This can also be seen in the results of sections 5.1 and 5.2. However, there are also real synergies among systems, produced by genuine efficiency gains. In this analysis is difficult to separate the share of benefits caused by each type of synergies. Therefore, as future work, an analysis of such a scheme could be developed but with market participation, where all the considered systems buy and sell energy directly from the market (at the same energy price) instead of the conventional energy tariffs.

Although the study developed shows an example of synergies between urban systems, providing insights on the potential benefits that could be achieved, more analysis need to be done to additional case studies (to check how general these results are), or to find interactions and impacts between other technologies and systems. For instance, other commuting train services, electric buses, commercial facilities, etc., which in addition present different energy consumption patterns and new potential synergies.

Table 10
Savings of the case studies in comparison with the base case at different numbers of EVs.

Number of EVs	CS_{250DC}	CS_{250dC}	CS_{250Dc}
25	27.9%	9.3%	14.6%
100	27.6%	9.1%	14.5%
300	27.1%	8.8%	14.3%
500	25.9%	8.2%	12.7%
1000	22.1%	8.2%	9.4%
3000	15.0%	7.4%	7.2%
5000	11.3%	5.0%	5.9%

Table 11
Sensitivity analysis for metro energy profiles (total costs with 194 EVs and 250 × 4 households).

Parameter change	CS_{dcL} (M€)	CS_{DCL} (M€)	Change (%)
Original	42.90	31.08	27.57%
Metro profile −20%	39.93	29.17	26.94%
Metro profile +20%	45.88	33.00	28.07%
District energy price −20%	37.56	28.07	25.28%
District energy price +20%	48.24	33.13	31.33%
Metro energy price −20%	39.93	30.39	23.88%
Metro energy price +20%	45.88	31.23	31.92%

6. Conclusions

Synergies between urban systems are not always evident and their interactions are not always considered in the related literature. This paper provides an example of three interconnected systems, a residential district with distributed energy resources, EVs and metro, quantifying for different case studies how the systems can benefit from each other, revealing the underlying potential synergies.

The outcomes of this study show the high economic benefit that can be achieved by using the metro regenerative breaking and DER, but more importantly by interconnecting the systems, achieving a reduction of up to 30% on total costs. However, results suggest that metro system benefits more than the others in the interconnected scheme. Indeed, the metro takes advantage of the cheaper energy coming from the district via the EVs, due to the lower residential off-peak tariffs and the distributed generation. This phenomenon is due to the centralized optimization approach that minimizes the total cost of the complete system. Despite of being profitable, this approach can create additional energy and investment costs in some of the systems, endangering the possible benefit and/or willingness of the participants to join the interconnected scheme. An equilibrium problem, where each participant decides its investments and its operation optimizing its own benefit, could also be implemented as a more realistic approach.

Another interesting result is the EV saturation point for the proposed system, where extra EVs represent more load but do not provide additional useful storage to the system. This number can be relatively small when the energy transfer to the metro electrical substation is restricted, but it is also reduced by the presence of DER systems. Moreover, the overall cost reduction decreases with very large number of EVs, caused by the extra load of the EVs and the little or no use of the additional storage capacity. Both phenomena are important to consider at the planning level to maximize the benefit from the synergies between systems.

Finally, according to the case studies analysed and the sensitivity analysis developed, the input parameters that are more likely to have a significant impact on the results are the energy tariffs and DER costs, and in a lower degree, the metro energy profiles. Therefore, despite the potential difference on results under different urban contexts, the overall conclusions are likely to hold, as suggested by the results of the sensitivity analysis, showing the existence of synergies, both physical and opportunistic (created by different energy profiles or by different energy tariffs, respectively), between energy systems. Further research on this type of interconnected schemes will contribute to the creation of smarter and more interconnected cities.

Acknowledgment

The work of C. F. Calvillo was supported through an Erasmus Mundus Ph.D. Fellowship. The authors would like to express their gratitude to all partner institutions within the Erasmus Mundus Joint Doctorate Program in Sustainable Energy Technologies and Strategies (SETS) as well as to the European Commission for their support.

References

[1] C.F. Calvillo, A. Sánchez-Miralles, J. Villar, Energy management and planning in smart cities, Renew Sustain Energy Rev 55 (Mar. 2016) 273–287.
[2] J. Villar, I. Trigo, C.A. Diaz, P. Gonzalez, Cost-benefit analysis of plug-in electric vehicles penetration, In: European energy market (EEM), 2013 10th international conference on the, 2013, pp. 1–8.
[3] D.Jian Sun, Y. Zhang, R. Xue, Y. Zhang, Modeling carbon emissions from urban traffic system using mobile monitoring, Sci Total Environ 599 (Supplement C) (Dec. 2017) 944–951.
[4] J. García-Villalobos, I. Zamora, J.I. San Martín, F.J. Asensio, V. Aperribay, Plug-in electric vehicles in electric distribution networks: a review of smart charging approaches, Renew Sustain Energy Rev 38 (Oct. 2014) 717–731.
[5] I.J. Fernández, C.F. Calvillo, A. Sánchez-Miralles, J. Boal, Capacity fade and aging models for electric batteries and optimal charging strategy for electric vehicles, Energy 60 (Oct. 2013) 35–43.
[6] S. Beer, et al., An economic analysis of used electric vehicle batteries integrated into commercial building microgrids, IEEE Trans Smart Grid 3 (1) (2012) 517–525.
[7] U.B. Baloglu, Y. Demir, Economic analysis of hybrid renewable energy systems with V2G integration considering battery life, Energy Procedia 107 (Supplement C) (Feb. 2017) 242–247.
[8] J. Villar, C.A. Diaz, P. Gonzalez, F.A. Campos, Wind and solar integration with plug-in electric vehicles smart charging strategies, In: European energy market (EEM), 2014 11th international conference on the, 2014, pp. 1–6.
[9] A. González-Gil, R. Palacin, P. Batty, J.P. Powell, A systems approach to reduce urban rail energy consumption, Energy Convers Manag 80 (Apr. 2014) 509–524.
[10] A. González-Gil, R. Palacin, P. Batty, Sustainable urban rail systems: strategies and technologies for optimal management of regenerative braking energy, Energy Convers Manag 75 (Nov. 2013) 374–388.
[11] M. Peña-Alcaraz, A. Fernández, A.P. Cucala, A. Ramos, R.R. Pecharromán, Optimal underground timetable design based on power flow for maximizing the use of regenerative-braking energy, Proc Inst Mech Eng Part F J Rail Rapid Transit 226 (4) (Jul. 2012) 397–408.
[12] Á.J. López-López, R.R. Pecharromán, A. Fernández-Cardador, A.P. Cucala, Assessment of energy-saving techniques in direct-current-electrified mass transit systems, Transp Res Part C Emerg Technol 38 (Supplement C) (Jan. 2014) 85–100.
[13] ElEconomistaES, Metro de Madrid recargará coches eléctricos gratis con su energía de frenado (Madrid's metro recharges EVs for free with its regenerative braking energy). [Online]. Available: http://goo.gl/wIJB2P. [Accessed 18 Apr 2017].
[14] S. Su, T. Tang, Y. Wang, Evaluation of strategies to reducing traction energy consumption of metro systems using an optimal train control simulation model, Energies 9 (2) (Feb. 2016) 105.
[15] M. Balamurugan, S.K. Sahoo, S. Sukchai, Application of soft computing methods for grid connected PV system: a technological and status review, Renew Sustain Energy Rev 75 (Aug. 2017) 1493–1508.
[16] D. Connolly, H. Lund, B.V. Mathiesen, M. Leahy, A review of computer tools for analysing the integration of renewable energy into various energy systems, Appl Energy 87 (4) (Apr. 2010) 1059–1082.
[17] C.F. Calvillo, A. Sánchez-Miralles, J. Villar, Assessing low voltage network constraints in distributed energy resources planning, Energy 84 (May 2015) 783–793.
[18] 'GAMS - Cutting Edge Modeling'. [Online]. Available: https://www.gams.com/. [Accessed 06 Jul 2017].
[19] CPLEX 12. [Online]. Available: https://www.gams.com/latest/docs/solvers/cplex/index.html. [Accessed 06 Jul 2017].
[20] K. Richa, C.W. Babbitt, G. Gaustad, X. Wang, A future perspective on lithium-ion battery waste flows from electric vehicles, Resour Conserv Recycl 83 (Feb. 2014) 63–76.
[21] Replacing EV Batteries: Your Costs Will Vary, PluginCars.com. [Online]. Available: http://goo.gl/j4Fu4u. [Accessed 26 May 2015].
[22] How much energy does a refrigerator use? - by Mr. Electricity. [Online]. Available: http://michaelbluejay.com/electricity/refrigerators.html [Accessed 25 Oct 2016].
[23] European Commission - Joint ResearchCentre, Photovoltaic Geographical Information System (PVGIS). [Online]. Available: https://goo.gl/6QagIh. [Accessed 28 Sep 2016].
[24] E. E. País, Metro reduce los trenes en tres de las líneas más usadas, EL PAÍS, 12-Apr-2009. [Online]. Available: http://elpais.com/diario/2009/04/12/madrid/1239535458_850215.html. [Accessed 03 Dec 2015].
[25] W. Carvajal-Carreño, A.P. Cucala, A. Fernández-Cardador, Optimal design of energy-efficient ATO CBTC driving for metro lines based on NSGA-II with fuzzy parameters, Eng Appl Artif Intell 36 (Nov. 2014) 164–177.
[26] Metro de Madrid (Madrid's metro), Line 3 Time Schedule. [Online]. Available: https://goo.gl/C1h8sD. [Accessed 29 Sep 2016].
[27] Google Maps, 'Madrid', Madrid. [Online]. Available: https://goo.gl/OXkL24. [Accessed 29 Sep 2016].
[28] M. Domínguez, A. Fernández-Cardador, A.P. Cucala, R.R. Pecharromán, Energy savings in metropolitan railway substations through regenerative energy recovery and optimal design of ATO speed profiles, IEEE Trans Autom Sci Eng 9 (3) (Jul. 2012) 496–504.
[29] Ayuntamiento de Madrid (Madrid City Council), Aparcamientos municipales (municipal parking lots). [Online]. Available: http://goo.gl/ihYlD2. [Accessed 29 Sep 2016].
[30] Eight Tips to Extend Battery Life of Your Electric Car, PluginCars.com. [Online]. Available: http://goo.gl/ExBCTW. [Accessed 18 Jun 2015].
[31] E. Schaal, M. Articles, and 2015 November 12, 10 Electric Vehicles With the Best Range in 2015, The Cheat Sheet.
[32] G. Pasaoglu Kilanc, et al., Driving and parking patterns of european car drivers – a mobility survey, european commission, EUR - scientific and technical research reports, 2012.
[33] Chevrolet Pressroom - United States - Spark EV, media.gm.com. [Online]. Available: https://media.gm.com/content/media/us/en/chevrolet/vehicles/spark-ev/2016.html. [Accessed 09 Sep 2016].
[34] M. Davis, Project sech-spahousec Análisis del consumo energético del sector residencial en España (Analysis of the energy consumption of the Spanish residential sector), Build Up, 25-Jan-2012. [Online]. Available: http://www.buildup.eu/en/node/23244. [Accessed 29 Sep 2016].
[35] How much do smart meters cost? - WeblogPost by Chris King, 01-May-2013, [Online]. Available: https://blogs.siemens.com/smartgridwatch/stories/957/, [Accessed 29 Sep 2016].
[36] REE, 'Proyecto INDEL - Atlas de la demanda eléctrica española INDEL proyect - atlas of the Spanish electric demand)'. [Online]. Available: https://goo.gl/6g4Xjg. [Accessed 29 Sep 2016].
[37] C.F. Calvillo, A. Sánchez-Miralles, J. Villar, F. Martín, Optimal planning and operation of aggregated distributed energy resources with market participation, Appl Energy 182 (Nov. 2016) 340–357.
[38] Iberdrola, Residential time-of-use electric tariff. [Online]. Available: https://www.iberdrola.es/home/electricity [Accessed 29 Sep 2016].
[39] Iberdrola, 'Residential gas tariff'. [Online]. Available: https://www.iberdrola.es/home/gas/home-gas-plan. [Accessed 18 Apr 2017].
[40] L. N. España, 'El desglose de la factura de la luz'. [Online]. Available: http://www.lne.es/economia/2014/02/07/desglose-factura-luz/1539219.html. [Accessed 03 May 2016].
[41] 'Convocatorias de contratos públicos - Madrid.org - Portal de Contratación'. [Online]. Available: http://www.madrid.org/cs/Satellite?c=Page&cid=1109266544773&definicion=Contratos+Publicos&idOrganismo=1109266228042&idPagina=1204201624785&language=es&op2=Convocatoria+anunciada+a+licitaci%C3%B3n&pagename=PortalContratacion%2FPage%2FPCON_contratosPublicos&tipoServicio=CM_ConvocaPrestac_FA. [Accessed 29 Sep 2016].
[42] Endesa, 'High voltage commercial time-of-use electric tariff'. [Online]. Available: https://www.endesaclientes.com/companies/optimum-rate.html. [Accessed 29 Sep 2016].
[43] 'Distritos en cifras (Información de Distritos) - Ayuntamiento de Madrid'. [Online]. Available: http://www.madrid.es/portales/munimadrid/es/Inicio/El-Ayuntamiento/Estadistica/Distritos-en-cifras/Distritos-en-cifras-Informacion-de-Distritos-?vgnextfmt=default&vgnextoid=74b33ece5284c310VgnVCM1000000b205a0aRCRD&vgnextchannel=27002d05cb71b310VgnVCM1000000b205a0aRCRD. [Accessed 15 Sep 2016].